Supplementary Information

Functional gold nanoparticles coupled with microporous membranes: a flow controlled assay for colorimetric visualization of proteins

Yu-Yuan Chen,[a] Binesh Unnikrishnan,[a] Yu-Jia Li,[a] and Chih-Ching Huang*[abc]

[a]Institute of Bioscience and Biotechnology, National Taiwan Ocean University, 2, Pei-Ning Road, Keelung, 20224, Taiwan. E-mail: huanging@ntou.edu.tw; Tel.: +886-2-24622192 ext. 5517; Fax: +886-2-24622034

[b]Center of Excellence for the Oceans, National Taiwan Ocean University, Keelung, Taiwan

[c]School of Pharmacy, College of Pharmacy, Kaohsiung Medical University, Kaohsiung, 80708, Taiwan

Preparation of PG–AuNPs

PG, which is produced by *Streptococcal* bacteria and binds to the Fc region of hIgG, was attached to AuNPs (32-nm) through electrostatic and hydrophobic interactions. In brief, an AuNP solution (250 pM, 800 μL) was mixed with PG (1.0 μM, 40 μL) in sodium phosphate buffer (5.0 mM, pH 7.4) in a 1.5 mL tube. After a 2 h incubation at room temperature, the mixture was centrifuged (RCF of 15,000 g, 20 min at 4°C) to remove unattached PG. The supernatants were removed, and the oily precipitates were washed with 1.0 mL of 5.0 mM sodium phosphate buffer (pH 7.4). After three centrifugation/wash cycles, the colloid (PG–AuNPs) was resuspended in 1.0 mL of 5.0 mM sodium phosphate buffer (pH 7.4). From dynamic light scattering (DLS) measurements, we estimated the hydrodynamic diameters of the unlabeled AuNPs and PG–AuNPs assemblies to be 45.3 (±5.6; n = 4) and 57.8 (±6.3; n = 4) nm, respectively. The increased hydrodynamic size of the latter confirmed that PG molecules had self-assembled on the particle surfaces. The as-prepared PG–AuNPs were stable (no aggregation) in physiological buffer (25 mM Tris–HCl , 150 mM NaCl, 5.0 mM KCl, 1.0 mM $MgCl_2$, and 1.0 mM $CaCl_2$) for at least 2 weeks.

Preparation of Fib–AuNPs

To prepare the Fib–AuNPs (32-nm), AuNP (250 pM, 800 μL) solution was mixed with Fib (1.0 μM, 40 μL) in Tris–HCl buffer (20 mM, pH 7.4) in a 1.5 mL tube. After a 30 min reaction at room temperature, the mixture was centrifuged (RCF of 10,000 g, 20 min at 4°C) to remove unattached Fib. The supernatants were removed, and the oily precipitates were washed with 1.0 mL of 20 mM Tris–HCl buffer (pH 7.4). After three centrifuge/wash cycles, the colloid (Fib–AuNPs) was resuspended separately in 1.0 mL of 20 mM Tris–HCl buffer (pH 7.4). Relative to the bare AuNPs [45.3 (±5.6) nm; n = 4], the larger hydrodynamic diameters of the Fib–AuNPs [98.2 (±7.5) nm; n = 4] suggest that Fib molecules were adsorbed onto AuNPs.

Membrane-based colorimetric detection of hIgG

hIgG (0–75 nM) was equilibrated with PG–AuNPs (32-nm; 100 pM) in 0.5 mL of biological buffer in the presence of BSA (100 μM) for 10 min at room temperature. The mixture was 10-fold concentrated by centrifugation (RCF of 10,000 g, 20 min at 4°C) and the supernatant solutions (450 μL) were discarded. After vigorous vortexing (30 s) of the residual pellet solution (50 μL) on an orbital shaker, 5 μL of the solutions was separately dropped on NCM [1.0 cm (length) × 1.0 cm (width)] and then air dried for 20 min. The color intensity of the membranes was analyzed using Image J.

Membrane-based colorimetric detection of plasmin

Plasmin (0–20 nM) was equilibrated at room temperature with Fib–AuNPs (32-nm; 100 pM) in 0.5 mL biological buffer in the presence of BSA (100 μM) for 10 min. The mixtures were 10-fold concentrated by centrifugation (RCF of 10,000 g, 20 min at 4°C) and then the supernatant solutions (450 μL) were discarded. After vigorous vortexing (30 s) of the residual pellet solution (50 μL) on an orbital shaker, 5 μL of the resulting solutions was separately dropped on NCM [1.0 cm (length) × 1.0 cm (width)] and air dried for 20 min. The RGB values were recorded using Image J.

Sensing of hIgG by PG–AuNPs/NCM

We further applied PG–AuNPs coupled with NCM (pore size, 0.45 μm) to detect hIgG (Mw, approximately 150 kDa) in the biological buffer in the presence of BSA (100 μM). PG (derived from groups C and *G Streptococci*) preferentially binds to the Fc portion of IgG (binding affinity, $K = 10^8$–10^9 M^{-1}) from all four IgG subclasses (IgG1, 2, 3, and 4).[1,2] hIgG (≤25 nM) did not induce crosslinking aggregation of the PG–AuNPs, although PG comprises two Fc binding domains and can also interact with the Fab region of hIgG (Fig. S9, ESI†). The hIgG-induced crosslinking aggregation was probably suppressed by the nonspecific binding from the highly concentrated background BSA protein. However, the heavier IgG/PG–AuNPs complexes make the PG–AuNPs easily penetrate NCM, resulting in a large decrease in AuNP color on NCM. The G_{abs}/G_{abs}^0 ratios of the images for various concentrations of hIgG are given in Fig. S11. The descriptors G_{abs} and G_{abs}^0 represent the green component absorbance of the PG–AuNPs/NCM

probe in the absence and presence of hIgG. The PG–AuNPs/NCM probe allowed the detection of hIgG at concentrations as low as 0.5 nM in the presence of 100 μM BSA. As indicated in Fig. S10 (ESI†), our PG–AuNPs/NCM probe selectively responded toward hIgG ions by a factor of ≥1,000-fold relative to other proteins.

Detection of plasmin by Fib–AuNPs/NCM

In a previous study, we demonstrated that Fib–AuNPs (32-nm) could be used as a colorimetric probe to detect plasmin based during plasmin-mediated cleavage of fibrinogen and induced the aggregation of AuNPs.[3,4] Plasmin is a trypsin-like serine protease that degrades insoluble fibrin to produce soluble fibrin degradation products.[5,6] Plasmin is produced in the fibrinolytic system from a proenzyme (plasminogen) through the action of plasminogen activator.[5,6] Fib (Mw, approximately 340 kDa) is a 45 nm-long disulfide-linked dimer of three nonidentical polypeptide chains (Aα, Bβ, and γ).[7,8] Relative to bare AuNPs, Fib–AuNPs exhibit high stability (no aggregation) in a biological buffer (data not shown). In the presence of plasmin (20 nM), the Fib molecules on the particle surfaces were cleaved, thereby decreasing particle hydrophilicity and minimizing steric effects. As a result, the aggregation of AuNPs occured and led to smaller and broader absorption bands (Fig. S12, ESI†). However, the sensitivity and dynamic range of this aggregation based Fib–AuNPs probe was poor based on the dose-response curve shown in Fig. S12. As demonstrated above for thrombin and hIgG, we further incorporated NCM as a substrate to colorimetrically detect plasmin using Fib–AuNPs. Fig. S13A shows the photographic responses of the Fib–AuNPs/NCM probe with different concentrations of plasmin. In the absence of plasmin, the Fib–AuNPs spread uniformly on NCM along with the buffer, exhibiting a uniform AuNP color. When Fib on the AuNPs was cleaved by plasmin, Fib–AuNPs had less affinity to NCM. In addition, the slightly aggregated Fib–AuNPs easily penetrated NCM. As a result, the color of the Fib–AuNPs on NCM decreased with increasing concentrations of plasmin (Fig. S13A). The G_{abs}/G_{abs}^0 values of Fib–AuNPs/NCM probe were plotted against the concentrations of plasmin (Fig. S13B) and suggested that the probe could detect 0–10.0 nM plasmin.

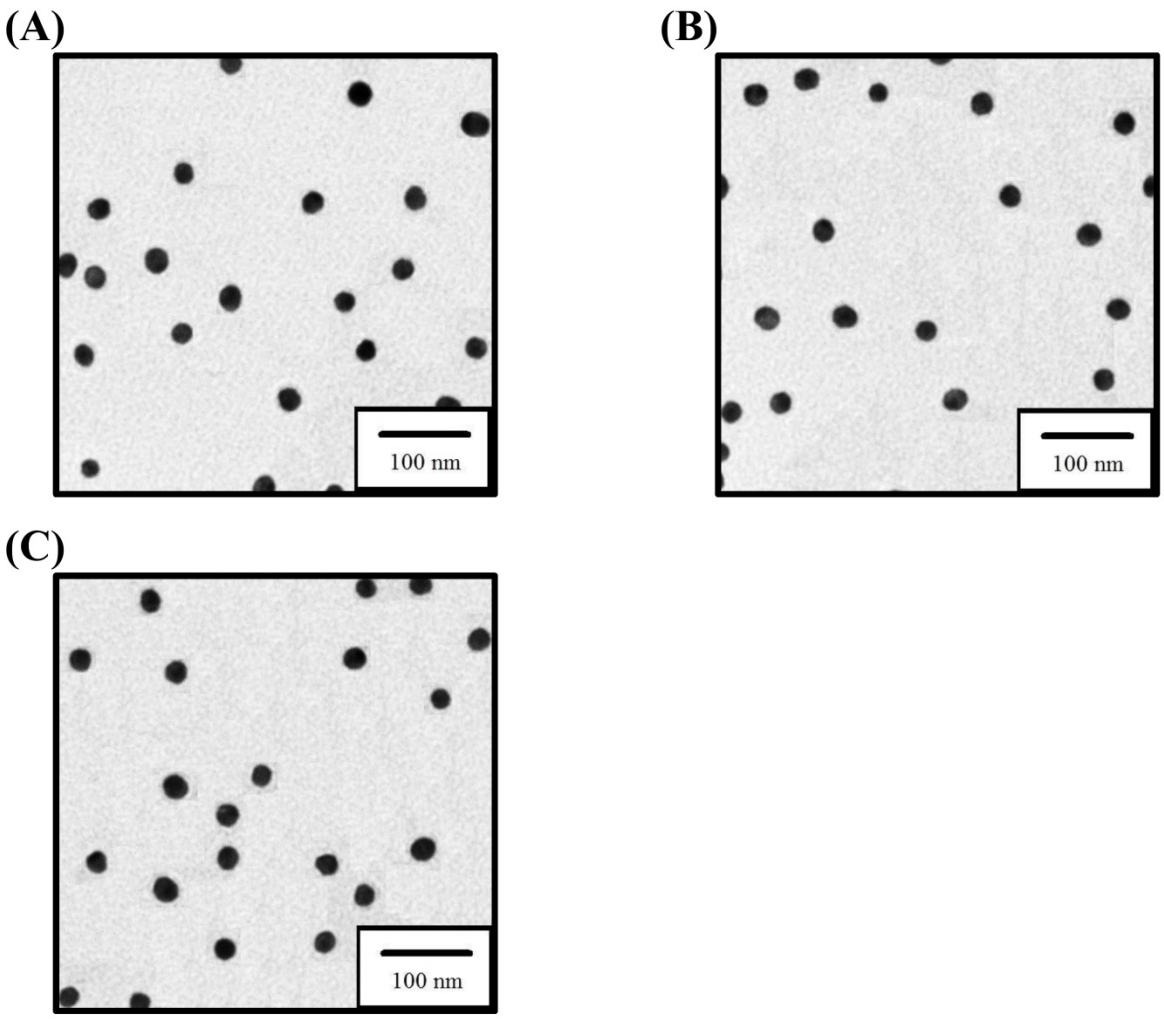

Fig. S1 TEM images of the as-synthesized (A) AuNPs (13-nm), (B) TBA_{29}–AuNPs, and (C) TBA_{29}–AuNPs in presence of thrombin (25 nM) in a biological buffer containing 100 μM bovine serum albumin.

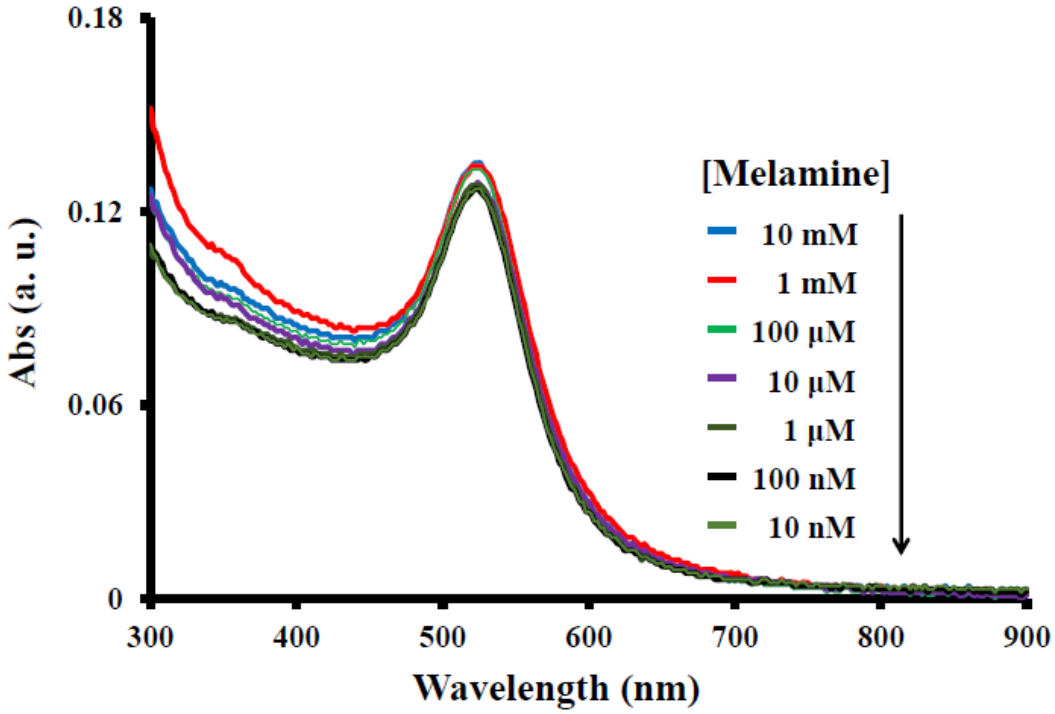

Fig. S2. UV-visible spectra of TBA_{29}–AuNPs (1 nM) in presence of different concentrations of melamine (10 nM to 10 mM) in Tris-HCl (pH = 7.4, 5 mM) buffer.

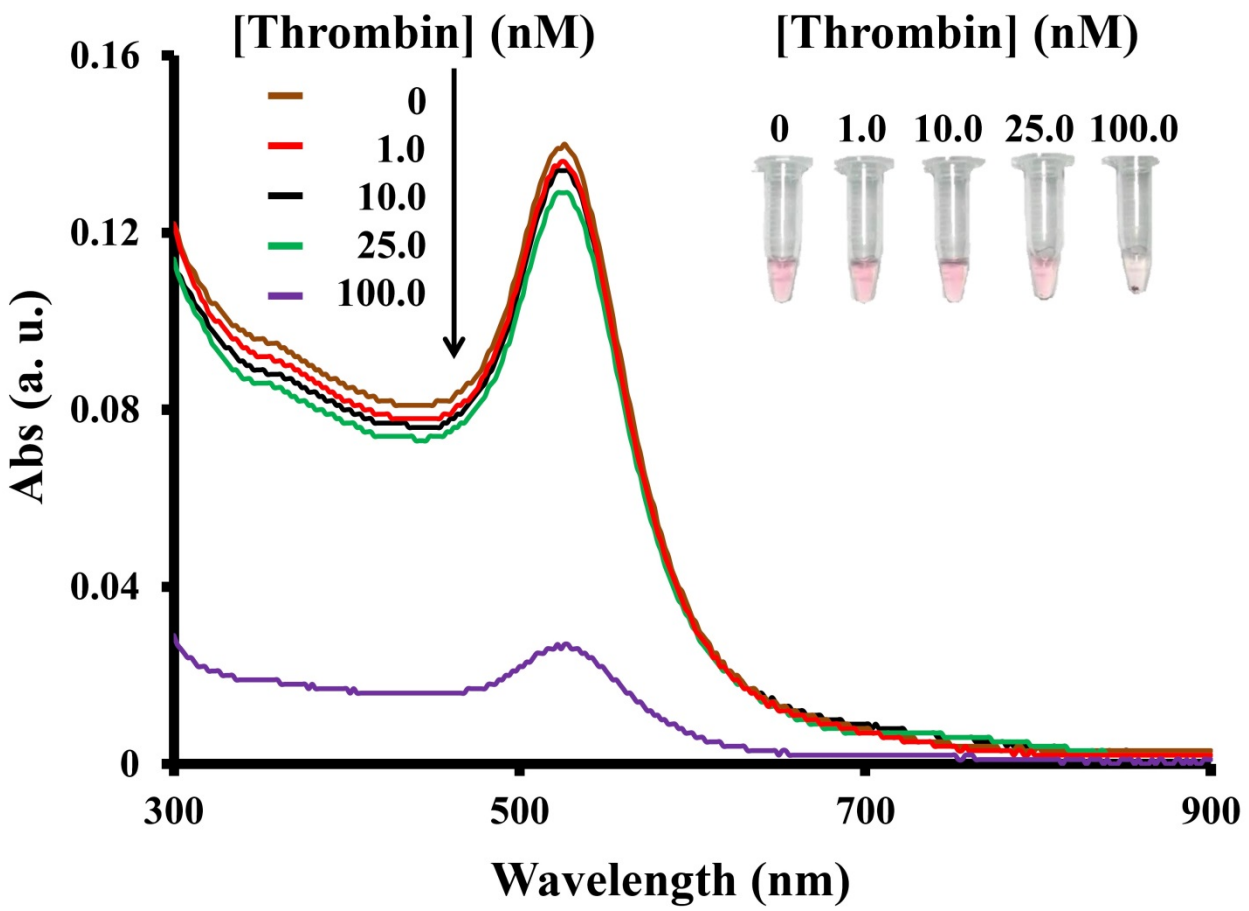

Fig. S3 UV–vis absorption spectra of TBA_{29}–AuNPs (1.0 nM) in the presence of thrombin (0–100.0 nM) in a biological buffer containing 100 μM bovine serum albumin. Inset: photographic images of the AuNP solutions. Absorbance (Abs) is plotted in arbitrary units (a. u.).

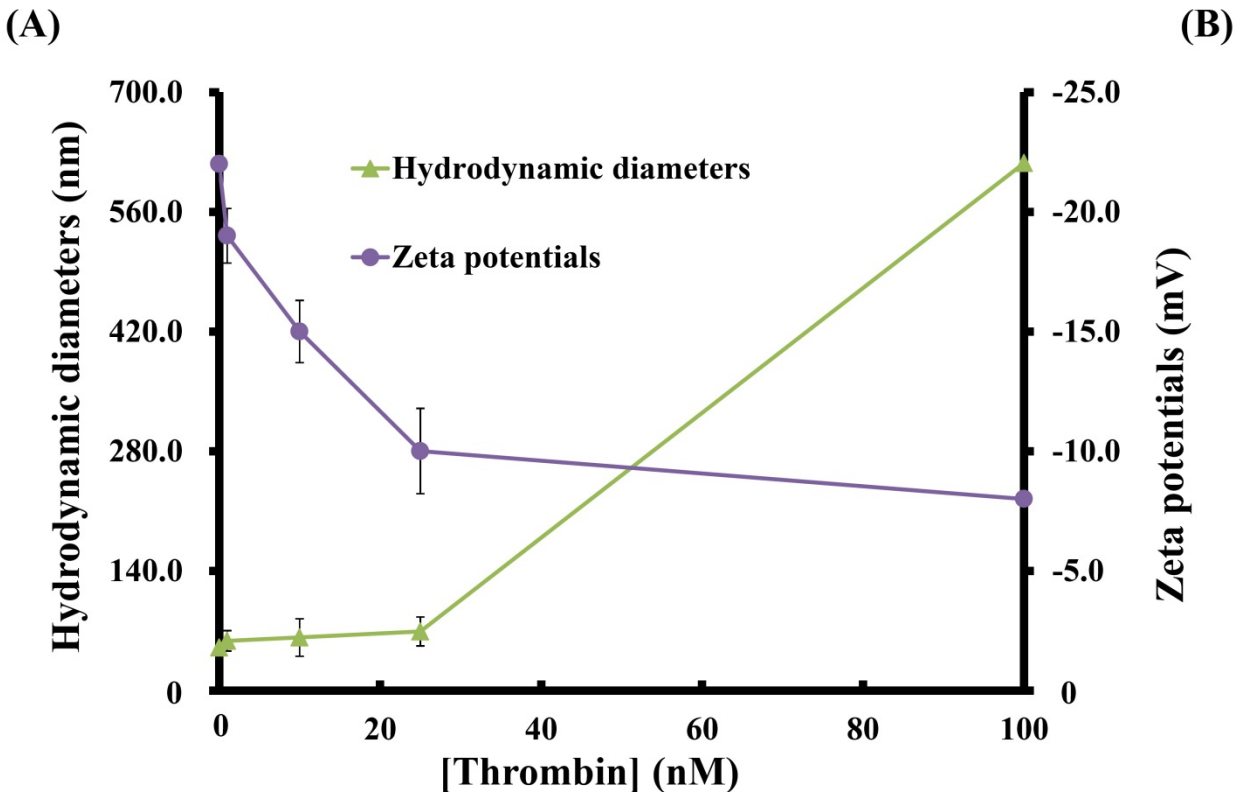

Fig. S4 (A) Hydrodynamic diameters and (B) zeta potentials (ζ) of TBA_{29}–AuNPs (1.0 nM) in a biological buffer containing 100 μM bovine serum albumin in the presence of thrombin (0–100.0 nM). Error bars represent standard deviations from three repeated experiments. Other conditions are the same as those described in Fig. S3.

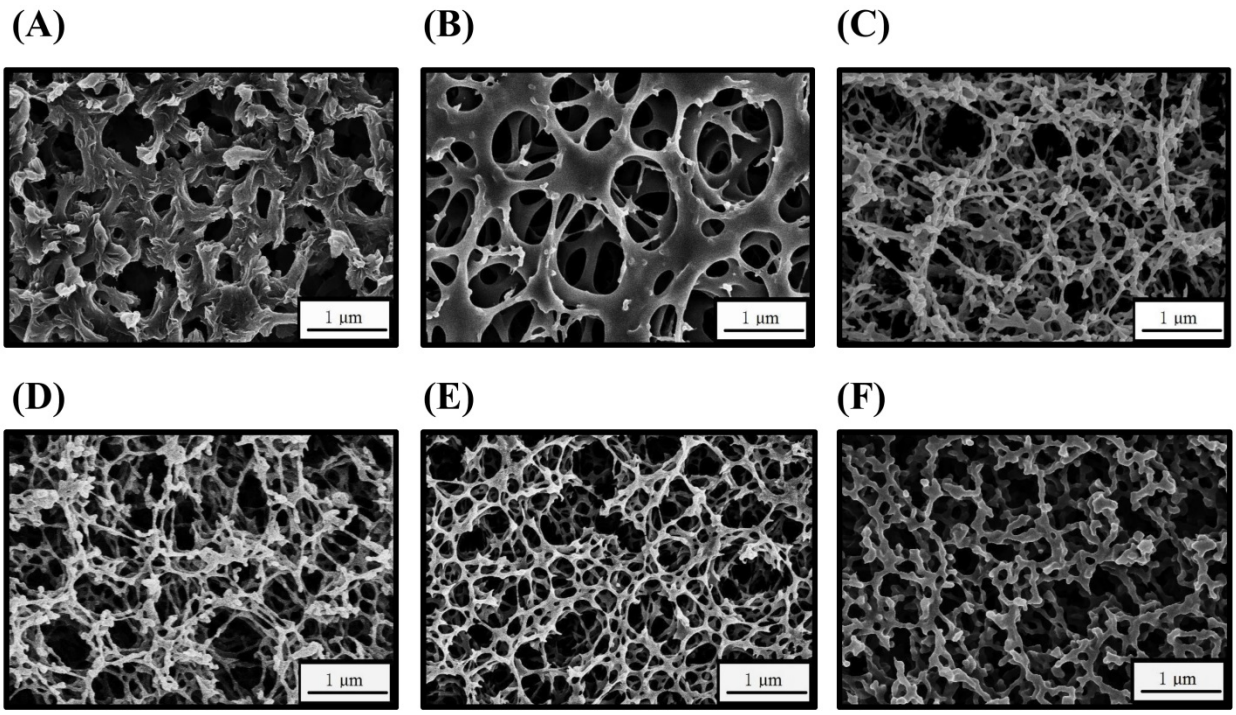

Fig. S5 Scanning electron microscopic images of (A) positively charged nylon transfer membrane (N^+M; 0.45 μm), (B) cellulose acetate membrane (CAM; 0.45 μm), (C) nitrocellulose membrane (NCM; 0.45 μm), (D) NCM (0.22 μm), (E) NCM (0.10 μm), and (F) mixed cellulose ester membrane (MCEM; 0.45 μm).

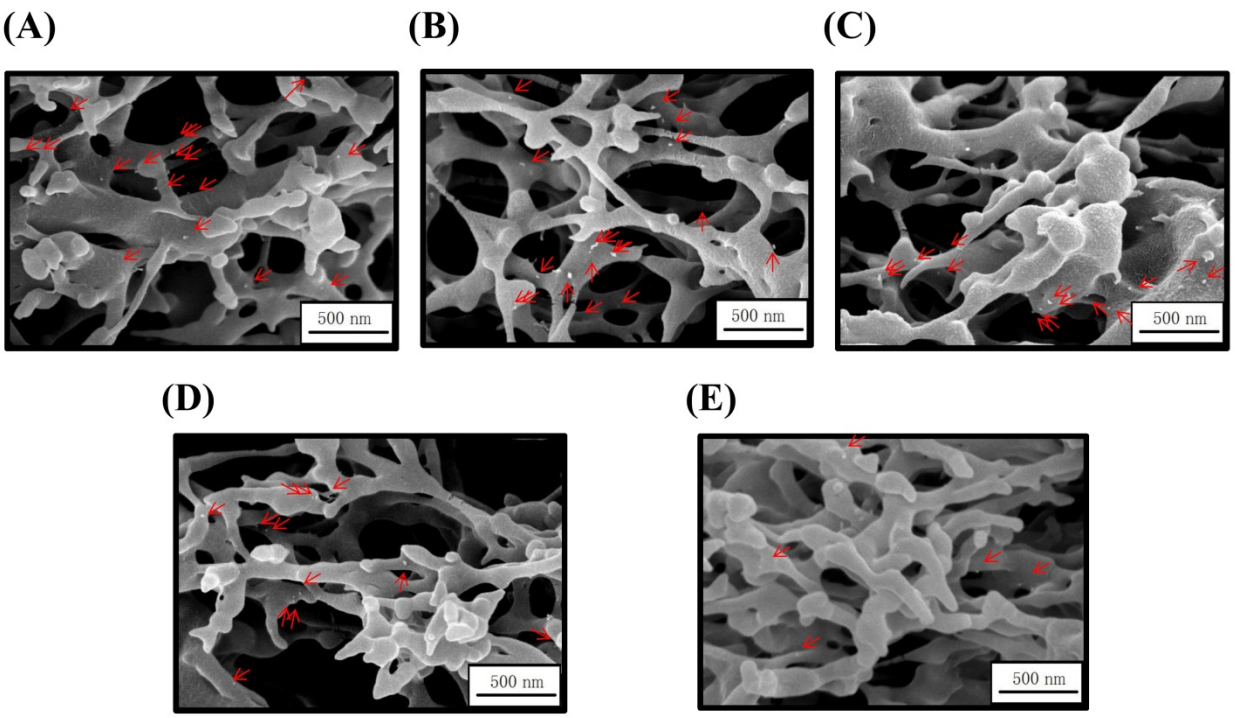

Fig. S6 Scanning electron microscopic images of the TBA_{29}–AuNPs/NCM in the (A) absence and (B–E) presence of thrombin (B) 2.5 nM, (C) 10.0 nM, (D) 25.0 nM, and (E) 100.0 nM. Other conditions are the same as those described in Fig. 1. Red arrows indicate AuNPs.

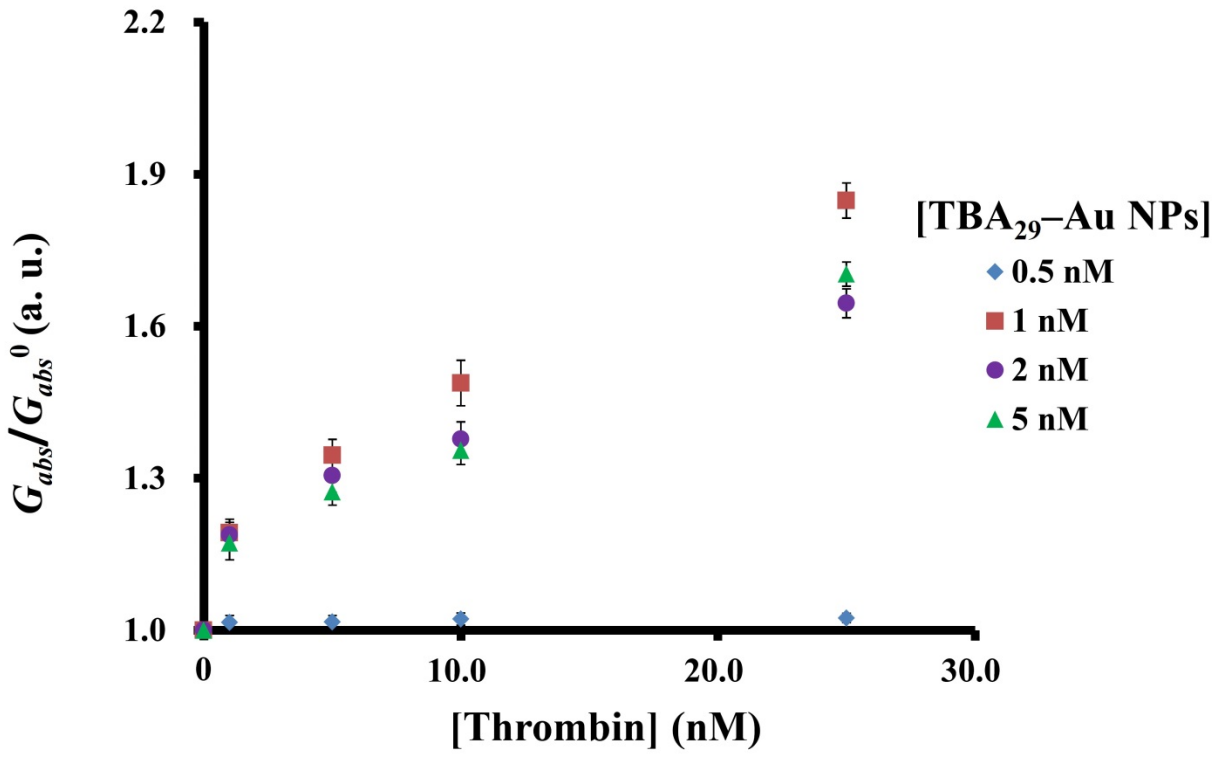

Fig. S7 G_{abs}/G_{abs}^{0} values of TBA_{29}–AuNPs/NCM for the determination of thrombin using different concentration of AuNPs from 0.5 – 5 nM in biological buffer containing 100 μM bovine serum albumin in the presence of thrombin (0–100.0 nM). Error bars represent standard deviations from three repeated experiments.

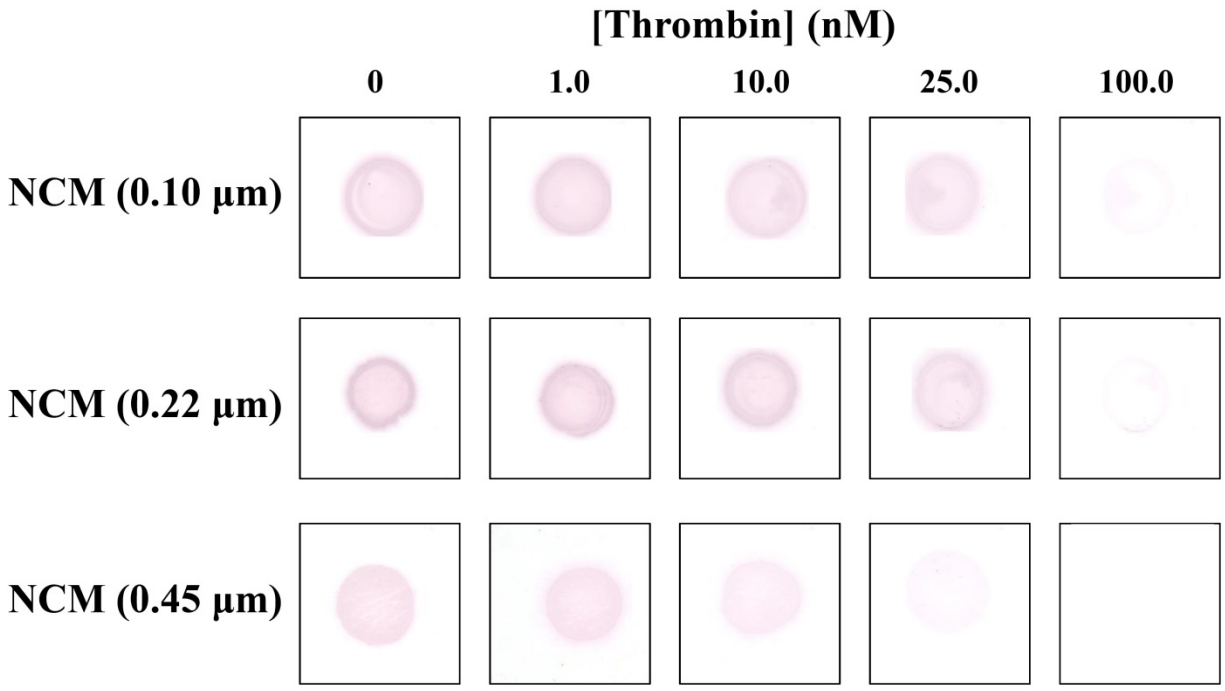

Fig. S8 Photographic images of TBA_{29}–AuNPs solution in the presence of different concentrations of thrombin (0–100.0 nM) after being dropped on a NCM with pore sizes of 0.10, 0.22, or 0.45 μm. Other conditions are the same as mentioned in Fig. 1.

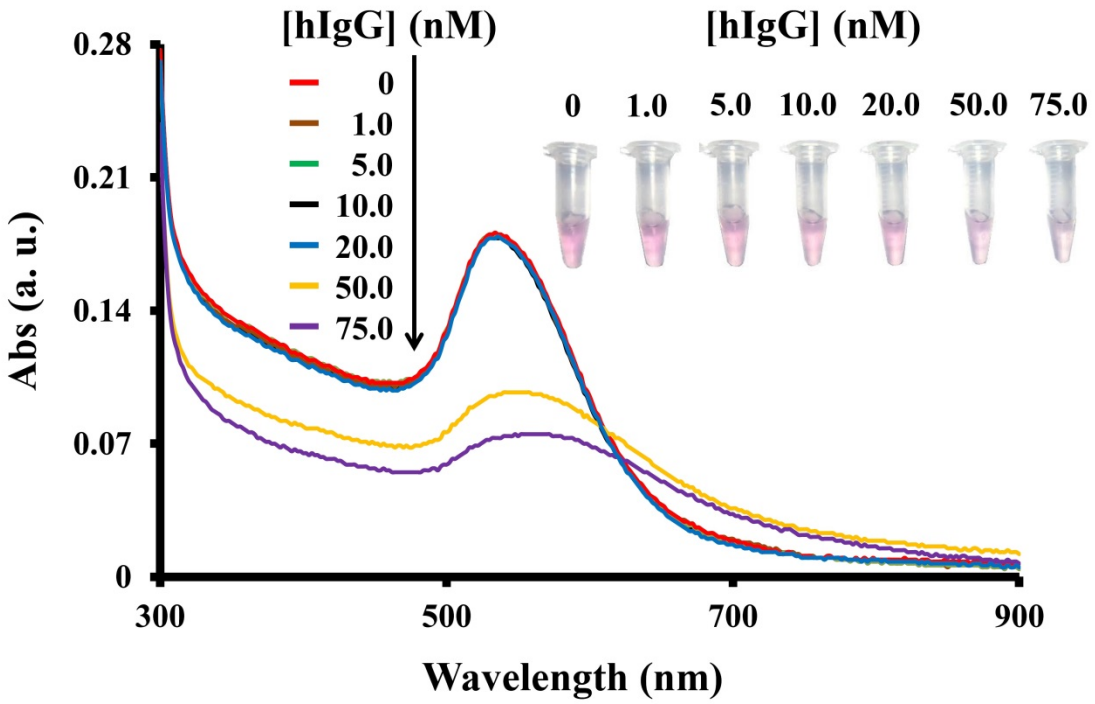

Fig. S9 UV–vis absorption spectra of PG–AuNPs (100 pM) in the presence of hIgG (0–75.0 nM) in biological buffer containing 100 μM bovine serum albumin. Inset: photographic images of AuNP solutions. Other conditions are the same as those described in Fig. S3.

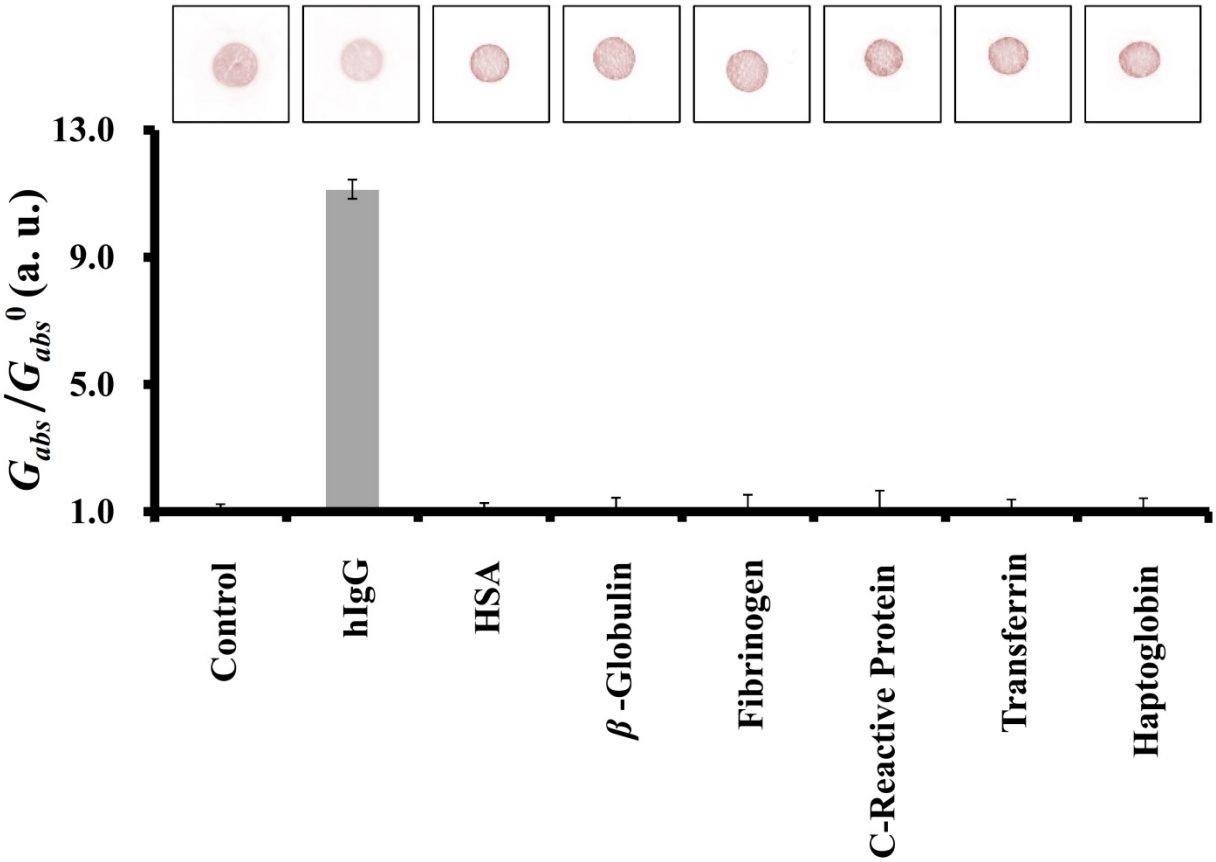

Fig. S10 Selectivity of the PG–AuNPs/NCM probe toward hIgG (10.0 nM) against other proteins (each 1.0 μM). Error bars for the G_{abs}/G_{abs}^{0} ratios represent standard deviations from three repeated experiments. Other conditions are the same as mentioned in Fig. 3.

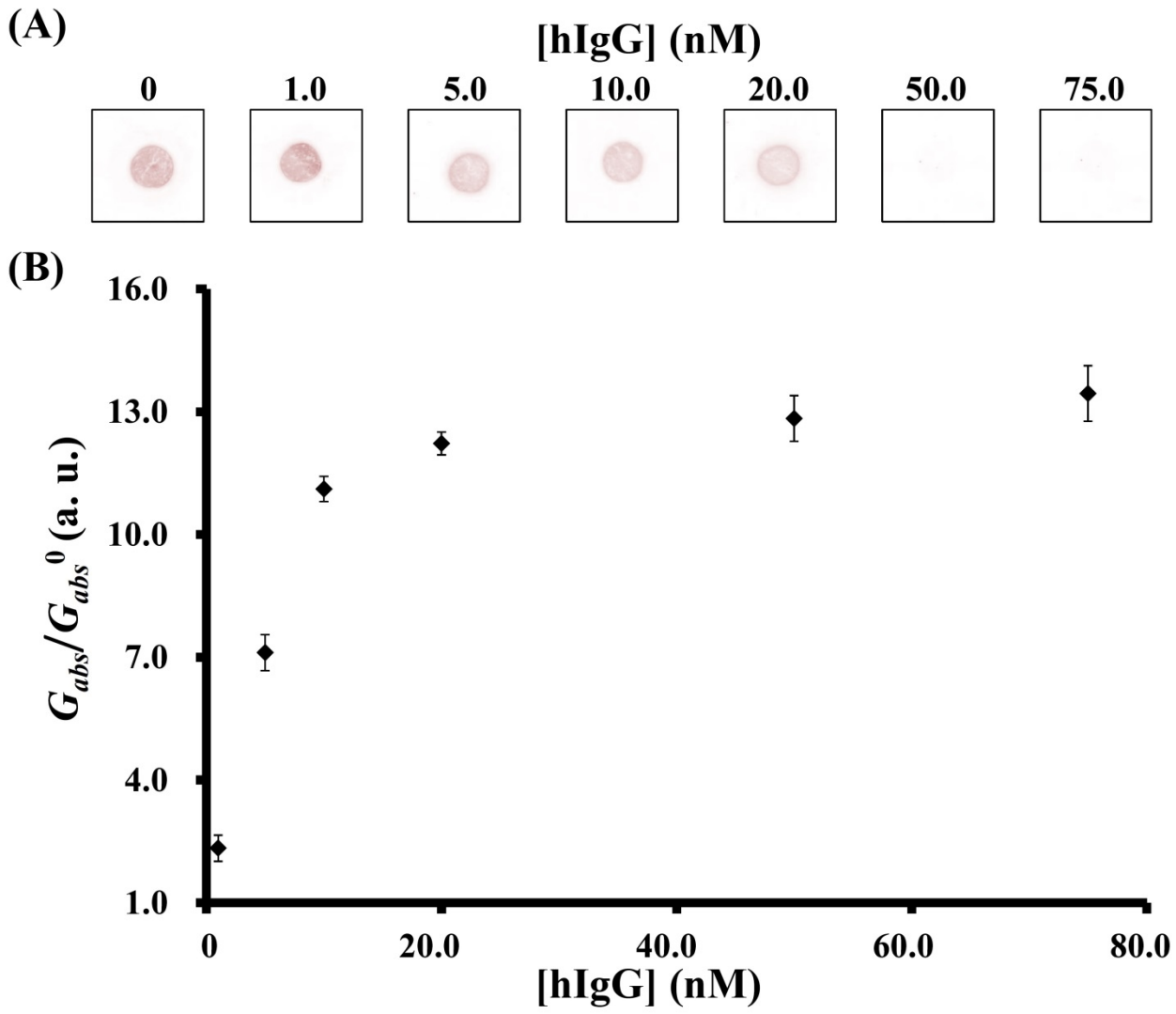

Fig. S11 (A) Photographic images of PG–AuNPs (100 pM) in the presence of different concentrations of hIgG (0–75.0 nM) after being dropped on a nitrocellulose membrane. (B) G_{abs}/G_{abs}^0 ratio of PG–AuNPs/NCM in the presence of hIgG (0–75.0 nM). Error bars in (B) represent standard deviations from three repeated experiments. Other conditions are the same as mentioned in Fig. 2.

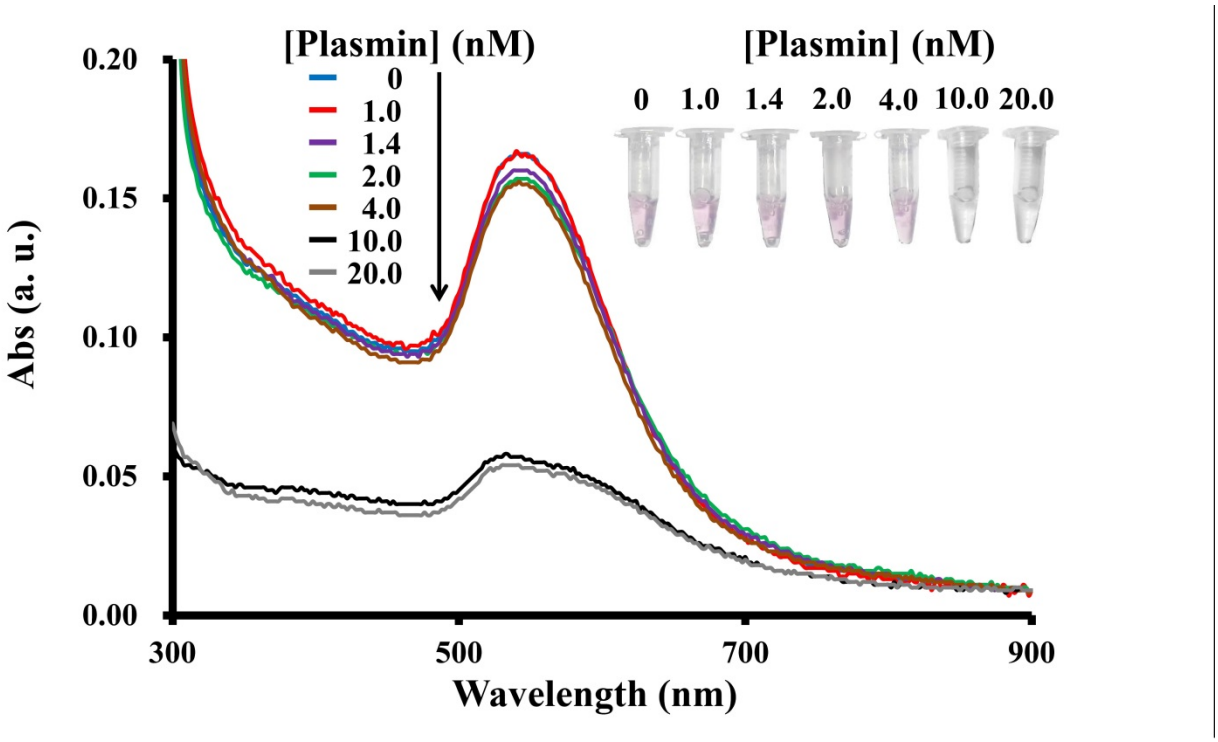

Fig. S12 UV–vis absorption spectra of Fib–AuNPs (100 pM) in the presence plasmin (0–20.0 nM) in biological buffer containing 100 μM bovine serum albumin. Inset: photographic images of AuNP solutions. Other conditions are the same as those described in Fig. S3.

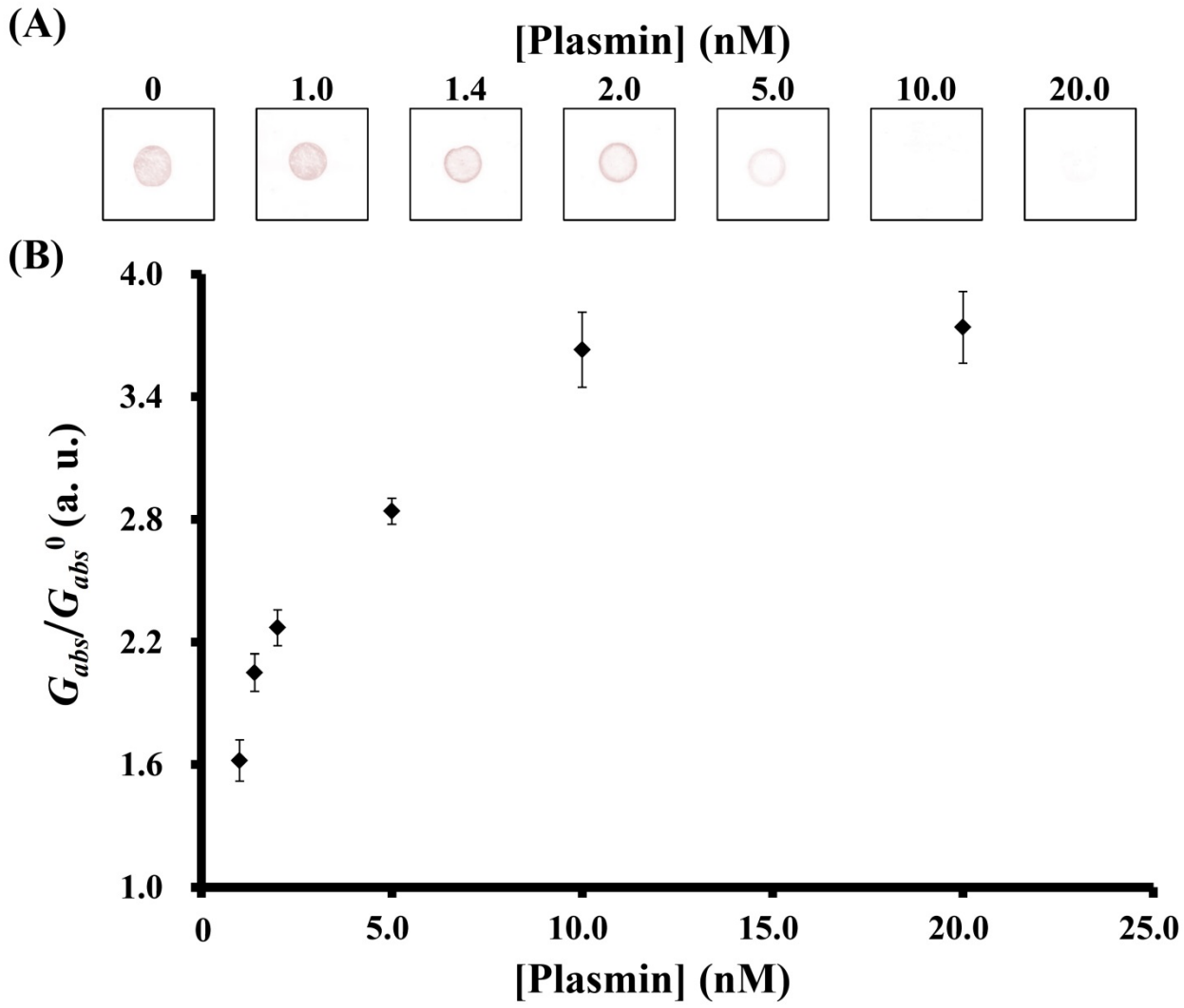

Fig. S13 Detection of plasmin (0–20.0 nM) in a biological buffer in the presence of 100 μM bovine serum albumin by the Fib–AuNPs/nitrocellulose membrane probe. Error bars in (B) represent standard deviations from three repeated experiments. Other conditions are the same as mentioned in Fig. S11.

Table S1 Comparison of sensing parameters of nanoparticle based colorimetric/fluorometric sensors for thrombin detection

Method	Probe	LOD	References
Colorimetric	TBA_{29}–AuNPs/NCM	0.3 nM	This Work
Colorimetric	TB/TBA/hemin complex(ABTS-H_2O_2)	0.5 nM	9
Colorimetric	TBA_{29}-Fe_3O_4@ AuNPs/TBA_{15}-Fe_3O_4@ AuNPs	1.0 nM	10
Fluorescence	FAM-Aptamer–AuNPs	10.0 nM	11
Mass Spectrum	Methylene Blue-ssDNA–AuNPs	16.0 nM	12

Table S2 Determination of thrombin concentrations in serum samples by TBA_{29}–AuNPs system.

Plasma Sample	**ELISA value mean ±SD (μM, n = 3)**	**FAuNP/NCM mean ±SD (μM, n = 3)**
Sample A	69.1 ± 0.5	54.5 ± 2.0
Sample B	74.6 ± 0.3	58.1 ± 2.0
Sample C	81.2 ± 0.6	62.9 ± 3.1
Sample D	84.1 ± 0.3	70.0 ± 4.2
Sample E	87.0 ± 0.3	74.7 ± 4.9
Sample F	107.9 ±0.4	85.8 ± 3.8

References

1 B. Guss, M. Eliasson, A. Olsson, M. Uhlén, A.-K. Frej, H. Jörnvall, J.-I. Flock and M. Lindberg, *EMBO J.*, 1986, **5**, 1567–1575.

2 U. Sjöbring, L. Björck and W. Kastern, *J. Biol. Chem.*, 1991, **266**, 399–405.

3 J.-W. Jian, W.-C. Chiu, H.-T. Chang, P.-H. Hsu and C.-C. Huang, *Anal. Chim. Acta*, 2013, **774**, 67–72.

4 W.-C. Chiu and C.-C. Huang, *Anal. Chem.*, 2013, **85**, 6922–6929.

5 F. J. Castellino and V. A. Ploplis, *Thromb. Haemostasis*, 2005, **93**, 647–654.

6 T. M. Gracés, A. Quijano and L. F. Arbeláez, *Iatreia*, 2013, **26**, 291–301.

7 R. F. Doolittle, *Ann. Rev. Biochem.*, 1984, **53**, 195–229.

8 S. T. Lord, *Curr. Opin. Hematol.*, 2007, **14**, 236–241.

9 D. Zhu, J. Luo, X. Rao, J. Zhang, G. Cheng, P. He, Y. Fang, *Anal. Chim. Acta*, 2012, **711**, 91–96.

10 G. H. Liang, S. Y. Cai, P. Zhang, Y. Y. Peng, H. Chen, S. Zhang, J. L. Kong, *Anal. Chim. Acta*, **2011**, *689*, 243–249.

11 J. Liu, Z. Guan, Z. Lv, X. Jiang, S. Yang, A. Chen, *Biosens. Bioelecteon*., 2014, **52**, 265–270.

12 J. C. Cunningham, N. J. Brenes and R. M. Crooks, *Anal. Chem.*, 2014, **86**, 6166–6170.